Tribol. Lubr., Vol. 36, No. 5 October 2020, pp. 290~296
Tribology and Lubricants

ISSN 2713-8011(Print) • 2713-802X(Online)
http://Journal.tribology.kr

DOI https://doi.org/10.9725/kts.2020.36.5.290

Molecular Dynamic Simulation for Penetration of Carbon Nanotubes into an Array of Carbon Nnantotubes

Ilkwang Jang[1] and Yong Hoon Jang[2†]

[1]*Research Professor, Dept. of Mechanical Engineering, Yonsei University*
[2]*Professor, Dept. of Mechanical Engineering, Yonsei University*

(Received August 31, 2020; Revised October 28, 2020; Accepted October 28, 2020)

Abstract – When two layers of carbon nanotube (CNT) arrays are loaded to mate, the free ends of individual CNTs come into contact at the interface of the two layers. This leads to a higher contact resistance due to a smaller contact region. However, when the free CNT ends of one array penetrate into the mating array, the contact region increases, effectively lowering the contact resistance. To explore the penetration of mating CNTs, we perform molecular dynamic simulations of a simple unit cell model, incorporating four CNTs in the lower array layer coupled with a single moving CNT on the upper layer. The interaction with neighboring CNTs is modelled by long-range carbon bond order potential (LCBOP I). The model structure is optimized by energy minimization through the conjugate gradient method. A NVT ensemble is used for maintain a room temperature during simulation. The time integration is performed through the velocity-Verlet algorithm. A significant vibrational motion of CNTs is captured when penetration is not available, resulting in a specific vibration mode with a high frequency. Due to this vibrational behavior, the random behaviors of CNT motion for predicting the penetration are confirmed under the specific gap distances between CNTs. Thus, the probability of penetration is examined according to the gap distance between CNTs in the lower array and the aspect ratio of CNTs. The penetration is significantly affected by the vibration mode due to the van der Waals forces between CNTs.

Keywords – carbon nanotube array, inter-nanotube interfaces, penetration, molecular dynamic simulation, vibration

1. Introduction

Carbon nanotubes (CNTs) are valued for their thermal conductivity, mechanical strength, and electrical conductivity. They have important roles in nanotech-nology, electronics, optics and other fields of materials science and technology. CNTs are also utilized as additives in nanoelectronics, sensors, and nanocomposites[1-4].

The mechanical properties of CNTs are superior because of their high elastic modulus (up to 1 TPa) and large tensile strength (126 GPa)[5]. In addition, their capacity for carrying electrical current density is 1000-fold that of Cu according to chirality[6]. These properties of CNTs can be used to enhance the function of materials that require electrical and mechanical properties simultaneously. However, although CNTs have good material properties for application in the field of nanotechnology, high contact resistance at the junctions of CNT devices has an adverse effect on the mechanical properties of CNTs. In addition, a variety of factors influence the contact resistance of CNTs including contact configuration, type of CNT, electrode material, fabrication process, and contamination status of the

† Corresponding author: Yong Hoon Jang
Tel: +82-2-2123-5812
E-mail: jyh@yonsei.ac.kr
https://orcid.org/0000-0002-5436-5465
https://orcid.org/0000-0002-4388-979X (IlKwang Jang)

contact surface[7].

Recently, contact resistance problems have been documented in some MEMS systems equipped with CNT arrays[8,9]. The array structure of CNTs intrinsically cannot be free of specific mechanical behaviors, such as bending or buckling. These behaviors have been investigated in detail in the literature[10-13]. Integration of CNTs may primarily affect the structural integrity and result in contact problems, specifically when CNTs with a high aspect ratio are formed[14,15]. Analysis of thermal contact resistance of a CNT array structure[16] revealed that integration of CNTs and their mechanical behaviors to understand the genuine characteristics of contact resistance yielded a complex system. Furthermore, the mechanical vibration and wave characteristics of the carbon nanotube array system can make the issues all the more complicated to understand the contact interaction of the CNT array system[17-19]. The contact interaction between CNTs in terms of nanoscale electronic transport is primary related to van der Waals forces occurring from the variation of potential energy[20].

A decrease in contact resistance in CNT structures would improve their electrical properties, and CNTs have the structural flexibility to create a large contact area. However, when two layers of CNT arrays are loaded to mate, the free ends of individual CNTs come into contact at the interface of the two layers. Thus, the free CNT ends of one array cannot penetrate into the mating array. It is conjectured that this phenomenon occurs because of strong van del Waals forces between neighbouring CNTs, a high aspect ratio, and the low bending stiffness of CNTs[16,21]. Motivated by the reported experimental evidence, we want to explore the possibility of improving the contact situation. If free CNT ends of one array penetrate into the mating array, the contact region between neighbouring CNTs would increase, leading to decreased contact resistance compared to the case where the free ends of individual CNTs come into contact at the interface of two CNT layers. It would be beneficial for designing the CNT array if we know the information of CNT diameter and the distance between CNTs in the array which the penetration of mating CNT is possible. Therefore, our objective in this work is to investigate the penetration of mating CNTs by establishing a simple unit cell model comprising four CNTs in the lower array layer coupled with a single moving CNT on the upper layer and performing molecular dynamic simulations.

This paper is organized as follows. A CNT array model and the simulation method are introduced in Section 2. In the Results and Discussion section, some characteristics of CNTs during the penetration are described and a possible explanation for penetration is provided. Several issues regarding the effect of gap distance between CNTs in the lower array and the effect of variation of aspect ratio of the CNTs on penetration are also considered.

2. Description of model and simulation method

We perform a molecular dynamics simulation to investigate penetration in a mating CNT array. The model is constructed by VMD 1.9.1[22] and analyzed by LAMMPS[23]. The array CNT model incorporates four CNTs in the lower array layer coupled with a single moving CNT on the upper layer, as shown in Fig. 1. The ends of the lower array layer are fixed and the moving CNT with a constant speed of V is directed to the center of the cross section in the lower array, moving until penetration is complete. The gap distance between the lower CNT array and the moving CNT, d, is designated as the cutoff distance for the

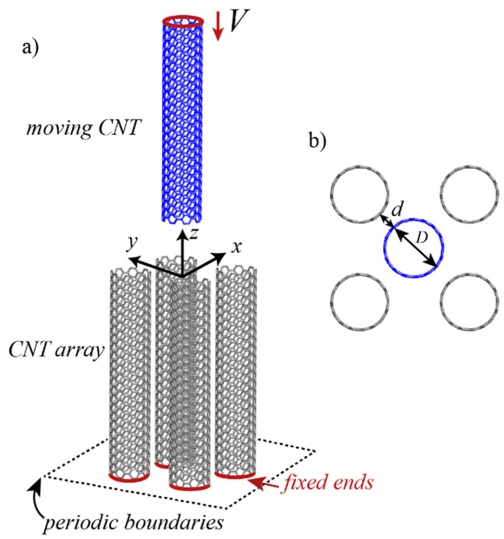

Fig. 1. Simulation model of (a) CNT array and moving CNT, and (b) section view with gap distance d between the CNT array and moving CNT.

simulation. The periodic boundary condition is applied along x and y direction of the outside cross section in the lower array.

Each CNT comprises a single walled armchair CNT with chiral vector of (8,8), showing good electrical conductivity. The diameter, D, and the longitudinal length of individual CNTs, L, are 10.84Å and 56.57Å, respectively, with an aspect ratio of 5.21[24]. In most simulations, this aspect ratio is kept constant. The number of atoms of each CNT is 768.

Although the aspect ratio of CNTs affects penetration, we restrict our analysis to a small aspect ratio. It is specifically known that an aspect ratio higher than 100 for a CNT results in bending, prohibiting the free CNT ends of one array from penetrating into the mating array. Thus, use of CNTs with a smaller aspect ratio increases the possibility of penetration, and van der Waals forces between CNTs can be considered in the absence of adhesion due to the long length of the CNTs.

Interaction with neighboring CNTs and covalent bonding of carbon atoms are modeled by long-range carbon bond order potential (LCBOP I)[24] with a cutoff distance of 2.2Å. This potential has been shown to be appropriate for CNT and fullerene simulations compared to the Lennard-Jones potential or reactive empirical bond order potential[25]. A specific LCBOP I potential is represented as

$$E_b = \frac{1}{2}\sum_{i,j}^{N} V_{i,j}^{tot} = \frac{1}{2}\sum_{i,j}^{N}\left(f_{c,ij} V_{ij}^{SR} + S_{sr,ij} V_{ij}^{LR}\right) \quad (1)$$

where the total pair interaction V_{ij}^{tot} is the sum of the short range part, $f_{c,ij}V_{ij}^{SR}$, and the long range part, $S_{ij}V_{ij}^{LR}$, and $f_{c,ij}$ is the smooth cutoff function and S_{ij} is the switching function, which have the relation of $S_{ij} = 1 - f_{c,ij}$.

The initial model structure is optimized by energy minimization through the conjugate gradient method. The effect of temperature on the CNT atoms is minimized by selection of a NVT ensemble, maintaining a temperature of 300 K during simulation. The time step in the transient analysis is less than 0.5 fs, which was chosen based on consideration of calculation time and accuracy. The time integration is performed by velocity-Verlet algorithm.

3. Results and Discussion

Penetration is determined by the gap distance d between CNTs in the lower array. If the gap distance d is large comparing with the diameter of CNT, interaction of the array CNT decreases, allowing penetration of the lower array CNT. Under a limited range of CNT's aspect ratio, the penetration phenomenon will be examined.

3-1. Characteristics of CNT during penetration

3-1-1. Variation of potential energy during penetration

When the moving CNT translates downward from the initial state and approaches the lower CNT array, a number of interactions between the lower array of CNTs and the translating CNT occur, including vibrations and mechanical bending. When the vertical distance between the free ends of the lower CNTs and the moving CNT approaches zero, we can determine whether penetration is possible or not. Severe interactions between CNTs in the lower array and the moving CNT induce vibrations from van der Waals forces[26]. This behavior results in variation of the horizontal gap distance between the lower CNT array and the moving one. Figure 2(a) shows penetration of the moving CNT into

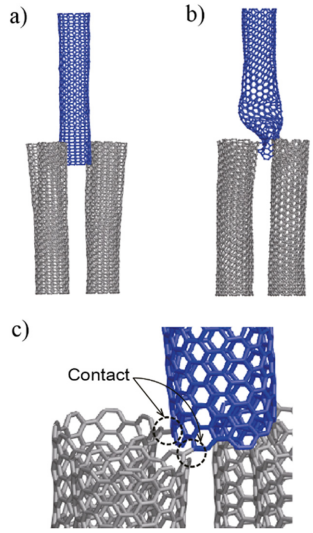

Fig. 2. Interaction between the lower CNT array and the moving CNT (a) when penetration is available, (b) when penetration is not available, (c) when adhesion of atoms occurs during no-penetration.

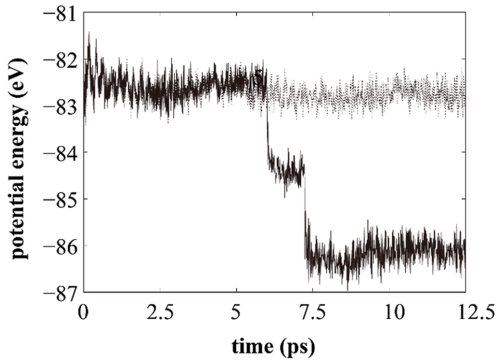

Fig. 3. Variation of potential energy allowed identification of penetration (dotted line) or no-penetration (solid line) for d = 1.80 Å and V = 9 m/s and d = 1.75 Å and V = 9 m/s, respectively.

the lower CNT array when the interaction is not severe. In the case of a severe interaction, the vibration amplitude extends beyond the gap distance d, indicating that the moving CNT came into contact or connected, as shown in Fig. 2(b). Another no-penetration interaction shows that the atoms between two CNTs are attracted to one another due to van der Waals forces and adhesion occurs, as shown in Fig. 2(c). After atom adhesion occurs, the CNTs bends drastically and then buckles, resulting in cessation of penetration.

To quantitatively define the conditions required for penetration, the potential energy of the moving CNT is investigated. Figure 3 shows the variation of potential energy when penetration into the CNT array is not available for the case of $d = 1.75$Å. When penetration is not possible, adhesion between the atoms of carbons occurred, leading to an abrupt change in potential energy. Thus, we estimate the change in potential energy associated with penetration, and confirm that penetration is not possible if the change in potential energy was greater than 3 eV. For the case of $d = 1.80$Å, the moving CNT penetrates into the CNT array and there is no large variation in the potential energy, as shown in Fig. 3.

3.1.2 Vibration frequency during penetration

To investigate the vibrational characteristics of CNT array during penetration, we calculate the total average of displacements for the group of atoms at the ends of the moving CNT at every time step. The total average of displacements is calculated as the root mean square of the displacements for x and y directions. Figures 4

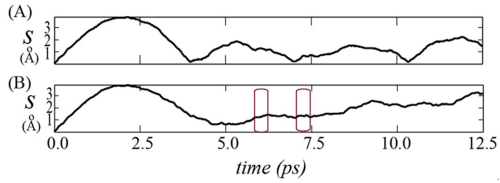

Fig. 4. Displacement response for (A) $d = 1.80$ Å and $V = 9$ m/s when penetration is available and for (B) $d = 1.75$ Å and $V = 9$ m/s when penetration is not available. For the case of (B), amplitudes at 6.01 ps and 7.235 ps are especially evident in the frequency range of 0.5 PHz ~1 PHz.

shows the responses of the total average displacement S at particular gap distance and velocity in the time domain for the existence and non-existence of penetration, respectively. In addition, the displacement signal is decomposed into several frequencies by using wavelet transformation[27]. Wavelet transformation provides a time–frequency decomposition framework that allows analysis of signals with a time-varying spectrum in which the time evolution of some components can be extracted in both amplitude and frequency. Specifically, signals are decomposed into several wavelet signals composed of an approximation signal an and detail signal d_j. Each wavelet signal shows time evolution of frequency components of the original signal within a specific frequency band. The sampling rates of each frequency band are

$$f(d_j) \in [2^{-(j+1)} f_s \sim 2^{-j} f_s](\text{Hz}), f(a_n) \in [0 \sim 2^{-(n+1)} f_s](\text{Hz}) \quad (2)$$

where f_s is the sampling rate of a sampled signal. We use the standard Matlab Wavelet Toolbox to perform discrete wavelet transformation of the signals, whereas Daubechies with an order of 10 is selected as the mother wavelet because higher order wavelets can detect fault signals[28]. The number of decomposition levels is set to 5 to detect the fault signal of no-penetration.

The displacement responses obtained for gap distances of 1.75Å and 1.8Å at the same speed of the moving CNT of $V = 9$ m/s are shown in Figures 5 and 6. The sampling rate for this response, f_s, is $2e^{15}$ samples/s. When penetration is possible, regular cycles of displacement motion with different amplitude are repeated. At the end of the cycle, the motion of the high-frequency range largely decays and low-frequency motion becomes dominant and then the end part of the moving CNT is

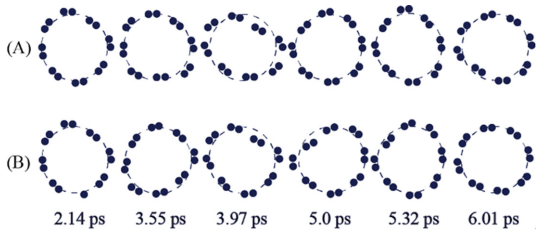

Fig. 5. Evolution of radial displacement of the moving CNT (a) when $d = 1.75$ Å and $V = 9$ m/s and (b) $d = 1.80$ Å and $V = 9$ m/s.

aligned to the vertical axis. This dominance of low frequency motion may be attributed to fixation or confinement of nanotubes by adhesion. This pattern of displacement motion is lost after the initial half cycle of motion, when penetration is not possible. Wavelet decomposition reveals two sharp peaks of amplitude at 6.01 ps and 7.235 ps, and these are especially evident in the frequency range of 0.5 PHz~1 PHz. The behavior of no-penetration is confirmed by the drop in potential during this period, as shown in Fig. 3.

To compare the vibrating motions of the moving CNT with and without penetration, we take snapshots of the radial displacement of the CNT as shown in Fig. 5. When the displacement response reaches its maximum amplitude in the initial cycle of displacement variation, i.e., t = 2.14 ps, the responses for the cases of penetration and no-penetration are the same, because the moving CNT was located far away from the interaction and only a little time has passed after relaxation process. As time evolves and reaches t=3.97 ps, severe deformations occur in both cases, but the magnitude of deformation for the case of no-penetration is larger. After that, the response for the case of penetration stabilizes and has an almost regular circle shape when penetration succeeds, while the response for no-penetration deviates from the circle shape at that instance. As mentioned above, a specific vibration mode with a certain frequency occurs when penetration is not available; in particular, a high frequency vibrating motion is noticed when penetration is not possible.

3.1.3 Effects of the gap distance between CNTs in the lower array

The characteristics of CNT array shows that dynamic behaviors are dominant according to the gap distance between CNTs in the lower array. This penetration behavior is sometimes unpredictable because the results change even under the same initial condition. To consider the randomness of penetration motion under the moving speed to downward direction ranging from 1 m/s to 30 m/s, the seed values for the initialization of speed are changed. For the gap distance, the availability of penetration is determined through 30 cases of simulations. In this simulation, the gap distance and the velocity of the moving CNT are varied from 1.5Å to 1.8Å and 1 m/s to 30 m/s, respectively. Then we seek the probability of penetration according to the gap distance between CNTs in the lower array. Fig. 6 shows the probability of penetration according to the normalized gap distance which is defined as d/D, where d and D are the gap distance and the diameter of CNT, respectively. The penetration is always possible when the normalized gap distance is above 0.1705. If the normalized gap distance decreases from 0.1705, the probability of penetration almost decrease monotonically. As the normalized gap distance d/D approaches 0.1382, the probability of penetration decreases to 40 %. If the normalized gap distance is below 0.1382, the penetration is not possible at all.

The effect of the gap distance between CNTs in the lower array in the penetration model is clarified when we consider interactions due to van der Waals forces according to the gap distance. When the gap distance d is small, penetration is not probable because the van der Waals forces are strong, inducing a large interaction between the lower array and the moving CNT. In the middle gap distance range, the possibility of penetration increases as the gap distance of CNTs increases. This coupling effect causes the CNT to have more complex movement. We notice that a specific vibration mode with a certain frequency occurs when penetration is not available as shown in Figure 5.

3.1.4 Effect of aspect ratio

In the previous simulation, the aspect ratio is kept constant, which means that both the longitudinal length and the radius of the cross section of the moving CNT do not change. However, previous studies[15,16] have hypothesized that a CNT array with a high aspect ratio could prohibit penetration of the moving CNT, because the high aspect ratio of the moving CNT would cause the ends of CNT to adhere to the CNT array, generating a bundle[15]. For relatively small aspect ratio of CNTs,

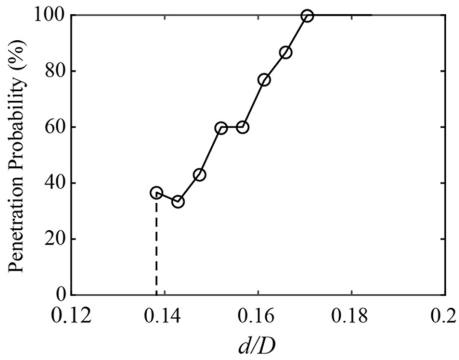

Fig. 6. Penetration probability according to gap distance between CNTs in the lower array, showing that the probability increases monotonically between *d*/*D* of 0.1382 and 0.1705.

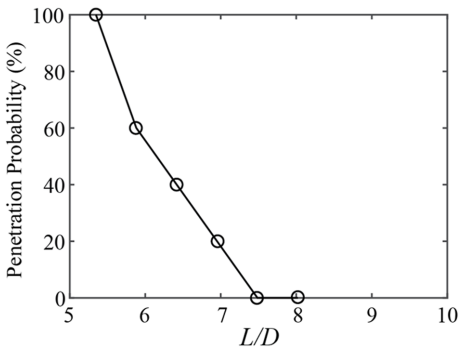

Fig. 7. Penetration probability according to aspect ratio, showing that the probability decreases monotonically as the aspect ratio increases.

the penetrating behavior of the CNT is being observed under some conditions. Thus, it is necessary to explore the degree of penetration behavior according to the aspect ratio.

In this molecular dynamic model, the length of CNTs varies from 56.57 Å to 84.86 Å and the diameter of CNTs is 10.84Å, resulting in the aspect ratio of 5.35 to 8.02. The gap distance between the moving CNT and the CNT array is 1.75Å. The simulation is performed by assigning 5 to 10 seed values for speed initialization at each aspect ratio. Figure 7 shows the penetration probability according to the aspect ratio. The aspect ratio is small below 5.35, the penetration always occurs. As the aspect ratio of CNTs increases, the probability of penetration decreases, approaching to zero when the aspect ratio is 7.49.

These outcomes show that as the aspect ratio of the CNTs forming the CNT array increases, the length of CNTs increases and the vibrational amplitudes of CNTs also increases. Thus, it is difficult to secure enough space for the moving CNTs to penetrate. In addition, the increase of aspect ratio for CNTs in the array gives rise to mechanical coupling between CNTs in the array expressed by the van der Waals forces between the moving CNT and the array CNTs with different lengths.

4. Conclusions

This investigation shows that penetration of mating CNTs is possible when the gap distance of CNTs between the moving part and the array layer is large under the limitation of a CNT configuration with a small aspect ratio. Penetration is significantly affected by the vibration mode due to van der Waals forces between CNTs. Our simulations are restricted to a simple unit cell model, but can be applied to design CNT structures with particular consideration of contact resistance.

Acknowledgements

This research was supported by the National Research Foundation of Korea (NRF) funded by the Korea government (MSIP) (Grant No. 2018R1A2B 6008891).

References

[1] T. Ahuja, D. Kumar, and others, “Recent progress in the development of nano-structured conducting polymers/nanocomposites for sensor applications,” *Sensors Actuators B Chem.*, Vol.136, No.1, pp.275-286, 2009.

[2] B. Sundaray, V. Subramanian, T. S. Natarajan, and K. Krishnamurthy, “Electrical conductivity of a single electrospun fiber of poly (methyl methacrylate) and multiwalled carbon nanotube nanocomposite,” *Appl. Phys. Lett.*, Vol.88, No.14, p. 143114, 2006.

[3] T. Zhang, S. Mubeen, N. V Myung, and M. A. Deshusses, “Recent progress in carbon nanotube-based gas sensors,” *Nanotechnology*, Vol.19, No.33, p.332001, 2008.

[4] Y. Xiao and C. M. Li, “Nanocomposites: from fabrications to electrochemical bioapplications,” *Electroanal. An Int. J. Devoted to Fundam. Pract. Asp. Electroanal.*, Vol.20, No.6, pp.648-662, 2008.

[5] R. S. Ruoff, D. Qian, and W. K. Liu, "Mechanical properties of carbon nanotubes: theoretical predictions and experimental measurements," *Comptes Rendus Phys.*, Vol.4, No.9, pp.993-1008, 2003.

[6] L. Jiang and L. Gao, "Carbon nanotubes- magnetite nanocomposites from solvothermal processes: formation, characterization, and enhanced electrical properties," *Chem. Mater.*, Vol.15, No.14, pp.2848-2853, 2003.

[7] B. Li *et al.*, "All-Carbon Electronic Devices Fabricated by Directly Grown Single-Walled Carbon Nanotubes on Reduced Graphene Oxide Electrodes," *Adv. Mater.*, Vol.22, No.28, pp.3058-3061, 2010.

[8] M.-O. Kim *et al.*, "Highly sensitive cantilever type chemo-mechanical hydrogen sensor based on contact resistance of self-adjusted carbon nanotube arrays," *Sensors Actuators B Chem.*, Vol.197, pp.414-421, 2014.

[9] J. Choi, Y. Eun, and J. Kim, "Investigation of interfacial adhesion between the top ends of carbon nanotubes," *ACS Appl. Mater. Interfaces*, Vol.6, No.9, pp.6598-6605, 2014.

[10] A. Cao, P. L. Dickrell, W. G. Sawyer, M. N. Ghasemi-Nejhad, and P. M. Ajayan, "Super-compressible foam-like carbon nanotube films," *Science (80-.).*, Vol.310, No.5752, pp.1307-1310, 2005.

[11] C. P. Deck, J. Flowers, G. S. B. McKee, and K. Vecchio, "Mechanical behavior of ultralong multi-walled carbon nanotube mats," *J. Appl. Phys.*, Vol.101, No.2, p.23512, 2007.

[12] J. Suhr *et al.*, "Fatigue resistance of aligned carbon nanotube arrays under cyclic compression," *Nat. Nanotechnol.*, Vol.2, No.7, pp.417-421, 2007.

[13] N. R. Paudel, A. Buldum, T. Ohashi, and L. Dai, "Modelling and simulations of adhesion between carbon nanotubes and surfaces," *Mol. Simul.*, Vol.35, No.6, pp.520-524, 2009.

[14] J. Li *et al.*, "Bottom-up approach for carbon nanotube interconnects," *Appl. Phys. Lett.*, Vol.82, No.15, pp.2491-2493, 2003.

[15] J.-H. Han, R. A. Graff, B. Welch, C. P. Marsh, R. Franks, and M. S. Strano, "A mechanochemical model of growth termination in vertical carbon nanotube forests," *ACS Nano*, Vol.2, No.1, pp.53-60, 2008.

[16] B. A. Cola, J. Xu, and T. S. Fisher, "Contact mechanics and thermal conductance of carbon nanotube array interfaces," *Int. J. Heat Mass Transf.*, Vol.52, No.15-16, pp.3490-3503, 2009.

[17] K. Kiani, "Wave characteristics in aligned forests of single-walled carbon nanotubes using nonlocal discrete and continuous theories," *Int. J. Mech. Sci.*, Vol.90, pp.278-309, 2015.

[18] O. Yilmazoglu *et al.*, "Vertically aligned multi-walled carbon nanotubes for pressure, tactile and vibration sensing," *Nanotechnology*, Vol.23, No.8, p.85501, 2012.

[19] M. X. Shi and Q. M. Li, "Mode transformation in single-walled carbon nanotubes," *Int. J. Mech. Sci.*, Vol.52, No.5, pp.663-671, 2010.

[20] A. Buldum and J. P. Lu, "Modeling and simulations of carbon nanotubes and their junctions on surfaces," *Appl. Surf. Sci.*, Vol.219, No.1-2, pp.123-128, 2003.

[21] H. Yoshida, T. Uchiyama, H. Kohno, and S. Takeda, "Environmental transmission electron microscopy observations of the growth of carbon nanotubes under nanotube--nanotube and nanotube--substrate interactions," *Appl. Surf. Sci.*, Vol. 254, No.23, pp.7586-7590, 2008.

[22] W. Humphrey, A. Dalke, K. Schulten, and others, "VMD: visual molecular dynamics," *J. Mol. Graph.*, Vol.14, No.1, pp.33-38, 1996.

[23] S. Plimpton, "Fast parallel algorithms for short-range molecular dynamics," *J. Comput. Phys.*, Vol.117, No.1, pp.1-19, 1995.

[24] N. Shun *et al.*, "Analysis of Three-Phase Structure of Epoxy Resin/CNT/Graphene by Molecular Simulation", *Polym.*, Vol.12, No.8, 2020.

[25] J. H. Los and A. Fasolino, "Intrinsic long-range bond-order potential for carbon: Performance in Monte Carlo simulations of graphitization," *Phys. Rev. B*, Vol.68, No.2, p.24107, 2003.

[26] K. Y. Xu, X. N. Guo, and C. Q. Ru, "Vibration of a double-walled carbon nanotube aroused by nonlinear intertube van der Waals forces," *J. Appl. Phys.*, Vol.99, No.6, p.64303, 2006.

[27] I. Daubechies, "The wavelet transform, time-frequency localization and signal analysis," *IEEE Trans. Inf. theory*, Vol. 36, No 5, pp.961-1005, 1990.

[28] Z. Hou, M. Noori, and R. S. Amand, "Wavelet-based approach for structural damage detection," *J. Eng. Mech.*, Vol.126, No.7, pp. 677-683, 2000.